

Pan-Arctic sea ice-algal chl *a* biomass and suitable habitat are largely underestimated for multiyear ice

Benjamin A. Lange^{1,2}  | Hauke Flores^{1,2} | Christine Michel³ | Justin F. Beckers⁴ | Anne Bublitz⁵ | John Alec Casey^{4,5}  | Giulia Castellani¹ | Ido Hatam^{6,7} | Anke Reppchen³ | Svenja A. Rudolph^{1,8} | Christian Haas^{1,5}

¹Alfred-Wegener-Institut Helmholtz-Zentrum für Polar- und Meeresforschung, Bremerhaven, Germany

²Zoological Institute and Zoological Museum, Biocenter Grindel, University of Hamburg, Hamburg, Germany

³Fisheries and Oceans Canada, Freshwater Institute, Winnipeg, MB, Canada

⁴Department of Earth and Atmospheric Sciences, University of Alberta, Edmonton, AB, Canada

⁵Department of Earth and Space Sciences and Engineering, York University, Toronto, ON, Canada

⁶Department of Biological Sciences, University of Alberta, Edmonton, AB, Canada

⁷Department of Chemical and Biological Engineering, University of British Columbia, Vancouver, BC, Canada

⁸Institute of Geography, University of Erlangen-Nuremberg, Erlangen, Germany

Correspondence

Benjamin A. Lange, Alfred-Wegener-Institut Helmholtz-Zentrum für Polar- und Meeresforschung, Bremerhaven, Germany. Email: benjamin.lange@awi.de

Funding information

Alberta Ingenuity Scholarship Programme, Grant/Award Number: RN:200700172; NSERC Discovery Grants, Grant/Award Number: 356589-08; Canadian Federal Programme on Energy Research and Development; Northern Scientific Training Program (NSTP); Circumpolar-Boreal Arctic Research (C-BAR) Programme; Helmholtz Association Young Investigators Group, Grant/Award Number: VH-NG-800; Alfred-Wegener-Institut; Helmholtz-Zentrum für Polar- und Meeresforschung; German Ministry of Economics Affairs and Energy, Grant/Award Number: 50EE1008, REKLIM-2013-04

Abstract

There is mounting evidence that multiyear ice (MYI) is a unique component of the Arctic Ocean and may play a more important ecological role than previously assumed. This study improves our understanding of the potential of MYI as a suitable habitat for sea ice algae on a pan-Arctic scale. We sampled sea ice cores from MYI and first-year sea ice (FYI) within the Lincoln Sea during four consecutive spring seasons. This included four MYI hummocks with a mean chl *a* biomass of 2.0 mg/m², a value significantly higher than FYI and MYI refrozen ponds. Our results support the hypothesis that MYI hummocks can host substantial ice-algal biomass and represent a reliable ice-algal habitat due to the (quasi-) permanent low-snow surface of these features. We identified an ice-algal habitat threshold value for calculated light transmittance of 0.014%. Ice classes and coverage of suitable ice-algal habitat were determined from snow and ice surveys. These ice classes and associated coverage of suitable habitat were applied to pan-Arctic CryoSat-2 snow and ice thickness data products. This habitat classification accounted for the variability of the snow and ice properties and showed an areal coverage of suitable ice-algal habitat within the MYI-covered region of 0.54 million km² (8.5% of total ice area). This is 27 times greater than the areal coverage of 0.02 million km² (0.3% of total ice area) determined using the conventional block-model classification, which assigns single-parameter values to each grid cell and does not account for subgrid cell variability. This emphasizes the importance of accounting for variable snow and ice conditions in all sea ice studies. Furthermore, our results indicate the loss of MYI will also mean the loss of reliable ice-algal habitat during spring when food is sparse and many organisms depend on ice-algae.

KEYWORDS

CryoSat-2, habitat classification, hockey stick regression, light transmittance, piecewise regression, sea ice algae, sea ice bio-optics, the Last Ice Area

This is an open access article under the terms of the Creative Commons Attribution-NonCommercial-NoDerivs License, which permits use and distribution in any medium, provided the original work is properly cited, the use is non-commercial and no modifications or adaptations are made.

© 2017 The Authors. *Global Change Biology* Published by John Wiley & Sons Ltd

1 | INTRODUCTION

The extent of multiyear sea ice (MYI) has declined dramatically during the satellite record from 75% of the total Arctic sea ice pack in the mid-1980s to 45% in 2011 (Maslanik, Stroeve, Fowler, & Emery, 2011). This trend is expected to continue, given the large sea ice volume losses recently observed from satellite ice thickness data (Laxon et al., 2013) and predicted by modelling studies (Schweiger et al., 2011). Furthermore, sea ice extent has been declining in all seasons with the most pronounced rates of decline in summer (Stroeve et al., 2011, 2012). The record minimum summer sea ice extent set in September 2012 (Parkinson & Comiso, 2013), which was a remarkable decline from the previous 2007 record, demonstrates the continued vulnerability of Arctic sea ice to continued climate change. In spite of the particular vulnerability of Arctic ecosystems to climate change, monitoring biological and biogeochemical processes and interactions is difficult as these components are not easily observed from satellites or airborne systems. Of great consequence to our understanding of the Arctic sea ice system is the paucity of ecologically relevant studies within the vast MYI-covered region of the Arctic Ocean (Wassmann, 2011; Wassmann, Duarte, Agusti, & Sejr, 2011).

A disproportional amount of research effort regarding sea ice ecology has been dedicated to coastal regions dominated by first-year sea ice (FYI). To understand and monitor Arctic changes, there is an urgent need to characterize biogeochemical processes associated with MYI. There is mounting evidence that MYI is a unique and important component of the Arctic sea ice system and has a more important ecological role than was previously assumed. For instance, Hatam, Lange, Beckers, Haas, and Lanoil (2016) suggested that a shift from a predominantly MYI to predominantly FYI sea ice cover will result in more functional instability within sea ice bacterial communities with potential consequences for nutrient dynamics in the Arctic marine environment. Furthermore, within the central Arctic Ocean during summer, regions dominated by MYI showed the highest proportion of ice-related primary production compared to the water column (Fernández-Méndez et al., 2015; Gosselin, Levasseur, Wheeler, Horner, & Booth, 1997). Under-ice-algal aggregate biomass (Katlein, Fernández-Méndez, Wenzhöfer, & Nicolaus, 2014) and maximum in-ice-algal biomass (Lange, Katlein, Nicolaus, Peeken, & Flores, 2016) were also observed within MYI-dominated regions compared to FYI-dominated regions. There remains a significant knowledge gap in terms of MYI-algal biomass and production during spring due to the logistical constraints of sampling within this region at this time of the year.

One approach to improve our understanding of the role of MYI-related ecosystems would be to identify key relationships between the algal biomass and the physical sea ice environment, which can be substantially different between MYI and FYI. Such relationships would improve our ability to model sea ice biogeochemical processes in MYI, identify important ecological thresholds and develop sea ice habitat classifications based on properties that are related to ice-

algal biomass, and which can apply to pan-Arctic satellite and airborne observations.

During spring, light availability is an important controlling factor of ice algae growth largely influenced by the physical properties of the snow and ice that control light transmittance to the bottom-ice (see review in Vancoppenolle, Bopp et al., 2013). Due to the influence of snow and ice on light transmission (Maykut & Grenfell, 1975; Thomas, 1963), snow and ice thickness have the potential to be used as proxies to identify regions of suitable sea ice-algal habitat. Threshold light levels (i.e., critical light levels) for ice-algal growth have been proposed and may be determined by laboratory experiments (Gosselin, Legendre, Demers, & Ingram, 1985; Gosselin, Legendre, Therriault, Demers, & Rochet, 1986). Therefore, we propose the physical environment may be a proxy of light availability for ice algae and empirical relationships can be used to establish a sea ice habitat classification.

A proxy for ice-algal growth was previously suggested by Lange et al. (2015) using snow and ice observations. Lange et al. (2015) conducted a multiyear study within the Lincoln Sea and demonstrated no significant differences between springtime MYI and FYI-algal chl *a* biomass. However, it was proposed that MYI hummocks (i.e., relatively large surface undulations protruding ~ 1 m above the adjacent level ice) may be suitable habitat for relatively high accumulations of algal biomass because of the typically lower snow cover on hummocks (<0.1 m), which could lead to higher light levels at the ice bottom, despite hummocks being thicker than the surrounding level ice. This hypothesis has potential pan-Arctic implications as snow-free/thin-snow hummocks are a common feature of MYI (Iacozza & Barber, 1999; Perovich et al., 2003; Sturm, Holmgren, & Perovich, 2002) and can represent large areas of suitable ice-algal habitat currently not accounted for in sea ice biomass estimates and modelling studies.

Here, we test the hypothesis that MYI hummocks have the potential for higher biomass than other ice types due to increased light transmission by providing statistically significant sampling efforts of MYI hummocks, MYI and FYI locations in the perennial ice zone. We further develop two observation-based habitat classification systems and apply them to pan-Arctic sea ice thickness and snow depth data, providing insights into the potential significance of MYI in terms of suitable ice-algal habitat on a pan-Arctic scale.

2 | MATERIALS AND METHODS

Here, we present observations and data collected in early May 2013 at two FYI stations and six MYI stations in the Lincoln Sea, north of Ellesmere Island, Canada (Figure 1). MYI dominates the ice coverage in this region; thus, FYI sites were less accessible and limited FYI sampling. These observations are supplemented with observations collected in 2010–2012 (see Lange et al., 2015). All sites visited from 2010 to 2013 are regrouped by location and shown in Figure 1. Groupings for 2012 and 2013 sites are listed in Table 1. Methods described in this study refer to sampling conducted during the 2013

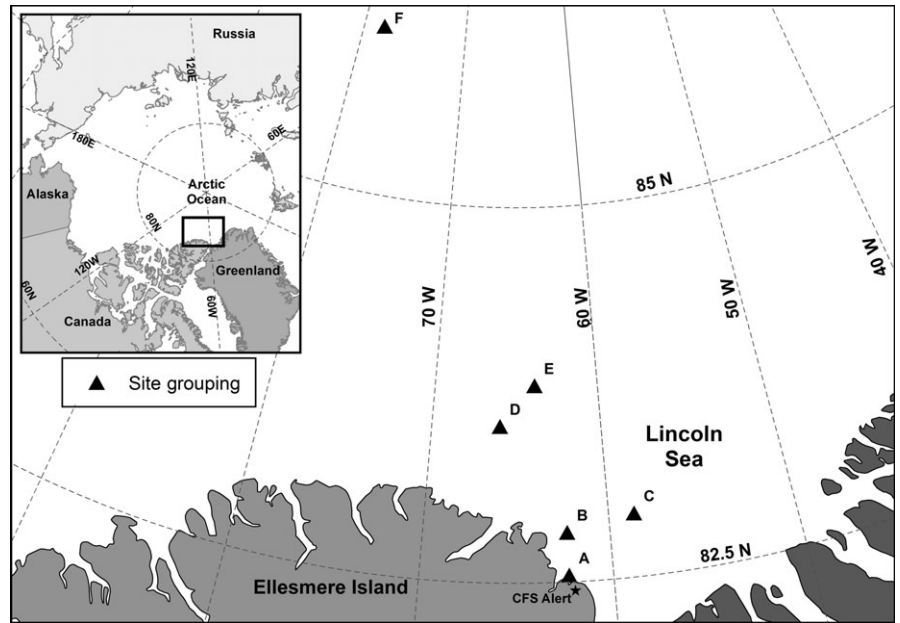


FIGURE 1 Map of the study region north of Ellesmere Island, Canada. Site groupings are shown, and the corresponding sites for each group are provided in Table 1

campaign unless otherwise stated. Site naming follows the same protocol as in Lange et al. (2015), in the form “SS-YY” with each two-digit site “SS” enumerated in consecutive order starting with “01” for each (2-digit) year “YY”.

2.1 | Light transmittance derived from snow and ice morphology measurements

Snow depth and ice thickness surveys were conducted consistent with surveys presented in Lange et al. (2015) and as described by Haas and Eicken (2001). In combination with the drill hole ice thickness measurements and snow depth surveys, measurements of the snow and ice surface elevation were conducted using a laser level and survey rod. The laser survey provided snow and ice surface elevation relative to the reference laser level plane and was conducted as described in Haas and Druckenmiller (2009). By tying these data in to sea ice freeboard measurements at the drill hole locations, the surface elevations were converted to relative elevations from the local sea surface height (i.e., the ice surface elevations represent sea ice freeboard). In 2012, the snow and ice surveys were conducted along a single transect at each site. During that year, survey transects were conducted along a MYI floe (site 01-12), a FYI floe (02-12) and at one site that spanned a MYI floe and a refrozen lead (05-12). Survey data from site 05-12 were split into two separate surveys at the boundary between the MYI floe and the refrozen lead. Survey transect lengths for each site are shown in Table 1. In 2013, the surveys were carried out along two perpendicular 100-m-long transects that intersected in the middle of each transect. In 2013, the snow and ice surveys were conducted on two FYI stations (02-13 and 03-13) and six MYI stations (01-13, 04-13, 05-13, 06-13, 07-13, 08-13; Table 1).

Coincident electromagnetic (EM) ice thickness surveys were conducted during the 2012 campaign using a Geonics EM31 (9.8 kHz,

3.66 m coil spacing) obtaining ice thickness values using an exponential fit method as described by Weissing, Lewis, and Ackley (2011). During the 2013 campaign, EM thickness surveys were conducted using a EMP-400 from GSSI (9 kHz, 1.21 m coil spacing). Results were obtained using a model analysis (2400 mS water conductivity) that finds the best fit between modelled and measured quadrature values, assigns the according ice thickness and averages data over 5-m intervals. Thickness values were then interpolated to 1-m intervals using the spline interpolation method provided by the R software function *spline* in the “stats” package.

Bulk optical thickness, k_B (dimensionless; i.e., the bulk extinction of light over the entire column of snow and ice), was calculated for the snow and ice surveys based on common literature values, symbolized hereafter as k_B . For all calculations, we used extinction coefficients for dry snow $k_s = 20.0 \text{ m}^{-1}$ and sea ice $k_i = 1.55 \text{ m}^{-1}$ (Grenfell & Maykut, 1977; Thomas, 1963). The value of k_s was chosen from a table of values (Thomas, 1963) based on a corresponding snow density comparable to measured values for our study region (Lange et al., 2015). The values of k_s and k_i were integrated over the depth of the corresponding ice and snow layers to provide optical thickness values (dimensionless) for all measurement locations along the survey transects and for each core site. k_B was then calculated as the sum of the optical thickness values for snow and ice. Larger values of k_B mean shallower penetration of light.

Following Nicolaus, Hudson, Gerland, and Munderloh (2010), transmittance (T) is defined as the ratio of the transmitted under-ice irradiance (E_T) to the incoming solar irradiance (E_S), taking the form:

$$T = E_T/E_S \tag{1}$$

Transmitted under-ice irradiance can be estimated by applying the Bouguer–Lambert law, according to the simple and widely used sea ice radiative transfer model (e.g., Grenfell & Maykut, 1977;

TABLE 1 Summary of sea ice survey sites from 2012 and 2013. Physical and optical properties of the sea ice and snow cover are provided for each site and summarized by ice class

Site	Group	Survey	Ice Class	h_i (μ) [m]		h_s (IQR)	fb (IQR)	rms _{fb}	T (IQR) %	T \geq 0.014% (CI) %		P ₁	P ₅	P ₁₀
				h_i (IQR)	h_s (IQR)					fb (IQR)	T (IQR) %			
05-12	A	Line (50 m)	5:FYI-Young	0.8	0.8 (0.8-0.8)	0.06 (0.04-0.09)	0.02 (-0.03 to 0.08)	0.08	1.8 (1.0-3.8)	100 (93-100)	-	-	-	-
02-12	A	Line (100 m)	3:FYI-Thick-Snow	1.8	1.8 (1.7-1.9)	0.29 (0.22-0.33)	0.11 (0.08-0.15)	0.12	0.0034 (0.0019-0.012)	24 (5-63)	-	-	-	-
02-13	A	Cross	4:FYI-Thin-Snow	1.7	1.8 (1.7-1.8)	0.17 (0.11-0.23)	0.11 (0.10-0.14)	0.12	0.12 (0.04-0.40)	94 (65-100)	31	30	39	
03-13	A	Cross	3:FYI-Thick-Snow	1.6	1.6 (1.5-1.7)	0.29 (0.24-0.38)	0.05 (0.02-0.07)	0.06	0.012 (0.0024-0.035)	48 (9-75)	27	45	25	
01-12	A	Line (400 m)	1:MYI-Thick	3.4	3.4 (2.9-3.8)	0.41 (0.24-0.53)	0.22 (0.07-0.44)	0.37	0.00000 (0.00000-0.00004)	5 (1-14)	-	-	-	-
05-12	A	Line (130 m)	nc	3	2.6 (2.2-3.8)	0.28 (0.21-0.36)	0.22 (0.14-0.44)	0.32	0.00050 (0.00010-0.0041)	10 (0-30)	-	-	-	-
01-13	A	Cross	2:MYI-Thin	2.9	2.7 (2.2-3.4)	0.31 (0.11-0.44)	0.14 (0.03-0.34)	0.29	0.00035 (0.00030-0.090)	39 (27-54)	24	20	25	
04-13	A	Cross	2:MYI-Thin	3.1	3.0 (2.4-3.6)	0.32 (0.14-0.43)	0.14 (-0.03 to 0.35)	0.27	0.00023 (0.00004-0.039)	33 (22-49)	21	25	23	
05-13	A	Cross	1:MYI-Thick	3.7	3.5 (3.1-4.2)	0.43 (0.29-0.64)	0.30 (0.02-0.43)	0.36	0.00010 (0.00000-0.0018)	10 (2-21)	24	10	10	
06-13	A	Cross	2:MYI-Thin	2.8	2.9 (2.3-3.2)	0.28 (0.17-0.42)	0.23 (0.05-0.35)	0.27	0.0053 (0.00050-0.033)	37 (21-59)	15	9	8	
07-13	A	Cross	2:MYI-Thin	2.5	2.5 (2.3-2.8)	0.33 (0.26-0.44)	0.21 (0.11-0.30)	0.27	0.0024 (0.00040-0.011)	22 (6-49)	14	9	6	
08-13	E	Cross	2:MYI-Thin	2.1	1.9 (1.8-2.5)	0.33 (0.24-0.43)	0.11 (0.06-0.18)	0.17	0.0044 (0.00050-0.0218)	35 (9-57)	23	23	8	
			1:MYI-Thick	3.5	3.4 (3.0-4.0)	0.42 (0.26-0.56)	0.26 (0.05-0.44)	0.36	0.0000 (0.00000-0.00070)	7 (2-16)	-	-	-	-
			2:MYI-Thin	2.7	2.6 (2.1-3.1)	0.32 (0.19-0.43)	0.16 (0.04-0.31)	0.26	0.00033 (0.00040-0.029)	33 (17-54)	-	-	-	-
			3:FYI-Thick-Snow	1.7	1.7 (1.6-1.8)	0.29 (0.24-0.36)	0.06 (0.04-0.10)	0.09	0.0076 (0.0020-0.028)	40 (8-71)	-	-	-	-
			4:FYI-Thin-Snow	1.7	1.7 (1.7-1.8)	0.17 (0.11-0.23)	0.11 (0.10-0.14)	0.12	0.12 (0.040-0.40)	94 (65-100)	-	-	-	-
			5:FYI-Young	0.8	0.8 (0.8-0.8)	0.06 (0.04-0.09)	0.02 (-0.03 to 0.08)	0.08	1.78 (1.0-3.78)	100 (93-100)	-	-	-	-

"Cross" surveys refer to surveys conducted along two perpendicular 100-m transects that intersect in the middle of each transect. μ refers to mean. Interquartile range (IQR) represents median (50th) and 25th - 75th percentiles.

h_i is the ice thickness; h_s is the snow depth; fb is the ice freeboard; rms_{fb} the root-mean-squared of the ice freeboard (i.e., proxy for surface roughness); T is the calculated transmittance from the snow and ice surveys. P₁, P₅ and P₁₀ are the patch sizes determined from autocorrelation analyses (Figs S9-S16) of ice thickness, snow depth and ice freeboard, respectively. nc refers to not-classified.

Katlein, Perovich, & Nicolaus, 2016; Katlein et al., 2015; Perovich, 1996), taking the form:

$$E_T = (1 - \alpha)E_S e^{-k_B} \quad (2)$$

Combining Equation (1) and (2), we can get:

$$T = (1 - \alpha)e^{-k_B} \quad (3)$$

where k_B is calculated as described above, and α is the surface albedo. Assuming predominantly diffuse incoming light conditions, we used values for α taken from Perovich (1996) for bare ice (0.70) or snow (0.81). To calculate transmittance for the core locations and the snow and sea ice surveys, we applied Equation (3) to the calculated k_B values and using the appropriate α value.

2.2 | Chl *a*

Sea ice core sampling and processing were conducted following procedures outlined in Lange et al. (2015). Chl *a* concentrations were determined fluorometrically using equations from Parsons, Maita, and Lalli (1989). Individual core sections were cut, then slowly melted and processed within 24 hr. Sample volumes between 50 and 250 ml were filtered onto Whatman GF/F 25-mm filters and extracted in 90% acetone at 4°C in the dark during 24 hr. The fluorescence was read on a Turner Design 10AU fluorometer calibrated with pure chl *a* extract (*Anacystis Nidulans*, Sigma Chemicals), prior and after acidification with 5% HCL (Parsons et al., 1989). We vertically integrated chl *a* (excluding phaeopigments) over the bottom section of each ice core, which varied in length between 0.1 and 0.2 m, hereafter referred to as the bottom-integrated chl *a* concentrations (mg/m²). Here, we used the bottom-integrated chl *a* concentrations presented in Lange et al. (2015) ($N = 18$) in addition to the nine cores collected in 2013 ($N = 27$). At one site, 06-13, ice cores were extracted from a refrozen pond (06-13-RP) and from an adjacent hummock (06-13-Hum). At this hummock site, three bottom-ice cores were sampled in order to assess the representativeness of ice cores from a MYI-hum site, which was important to test the hypothesis. We used the mean of these three cores as one sample for the statistical comparison between ice types (06-13-Hum).

2.3 | Statistical analyses

To identify a threshold value for suitable sea ice algae habitat, we used piecewise “hockey stick” regression (Toms & Lesperance, 2003; Toms & Villard, 2015) between the natural logarithm-transformed transmittance ($\ln[T]$) and chl *a* biomass for the ice core locations. Hockey stick regression identifies the change point value (i.e., threshold) of the calculated transmittance, which separates regions of high chl *a* biomass (hereafter referred to as suitable habitat) from regions of low chl *a* biomass (hereafter referred to as not-suitable habitat). Hockey stick regression tests if the samples were generated by two different regression equations, which are split at the change point, using a nonlinear least squares algorithm to test for model convergence. Here, we used a bootstrap sample size of 1000 and

calculated the 95% confidence intervals (CI). Hockey stick analysis was conducted using the *SiZer* package in R software version 2.15.2 (R-Development-Core-Team, 2012).

To test whether there were significant differences in bottom-ice-algal chl *a* biomass and calculated transmittance (T) between the different ice types, we performed an analysis of variance (ANOVA) applied to the log-transformed chl *a* and T observations. The different ice types included the following: younger refrozen lead ice (FYI-Young), older FYI (FYI), MYI with a refrozen melt pond (MYI-RP) and MYI hummocks (MYI-Hum). Log-transformations were conducted to conform with the assumptions of homogeneity in variance and a normal distribution. For a significant ANOVA test ($p < .05$), which indicated significant differences between ice types, we followed by post hoc Tukey HSD test to identify which ice types were significantly different ($p < .05$).

The 2013 snow and ice surveys were conducted in two perpendicular directions, west–east (WE) and south–north (SN). Each directional transect had a survey length of 100 m for a total survey length of 200 m per site. Snow depth, ice thickness, ice freeboard and T values were individually compared between the two survey directions at each site using a Student's *t*-test with a significance level of $p < .05$.

2.4 | Spatial autocorrelation analyses

Spatial autocorrelation was used to investigate the horizontal variability of sea ice thickness, snow depth and sea ice surface topography (i.e., sea ice freeboard). Autocorrelation was estimated using Moran's I (Legendre & Fortin, 1989; Moran, 1950), which was calculated for each of the eight sites at 30 equally spaced (3.3 m) distance classes between 2.65 and 98.35 m. Individual autocorrelation coefficients or Moran's I estimates were plotted for each distance class in the form of a spatial correlogram (Legendre & Fortin, 1989). All analyses were conducted using the “r” software function *correlog* from the “pgrmess” package. Autocorrelation coefficients for each distance class were assigned a two-sided p -value following methods in Ref (Legendre & Fortin, 1989), using a significance level of $p < .05$. We focused on the first x-intercept of the correlogram line (indicated by dashed vertical lines in Figure 2), which identifies the patch size, P , of the variables (Legendre & Fortin, 1989). In our case, patch sizes were identified for snow depth (P_s ; Figure 2a), ice thickness (P_i ; Figure 2b) and ice surface topography (P_{fb} ; Figure 2c). This methodology is consistent with spatial autocorrelation analyses used in other snow and sea ice studies to identify patch sizes of both biological and physical variables (e.g., Gosselin et al., 1986; Granskog et al., 2005; Rysgaard, Kühl, Glud, & Hansen, 2001; Sjøgaard et al., 2010).

2.5 | Pan-Arctic sea ice algae habitat classification system

For the pan-Arctic habitat classification, we used the CryoSat-2 sea ice thickness data product of Ricker, Hendricks, Helm, Skourup, and Davidson (2014). Snow depth values are included in the Ricker et al.

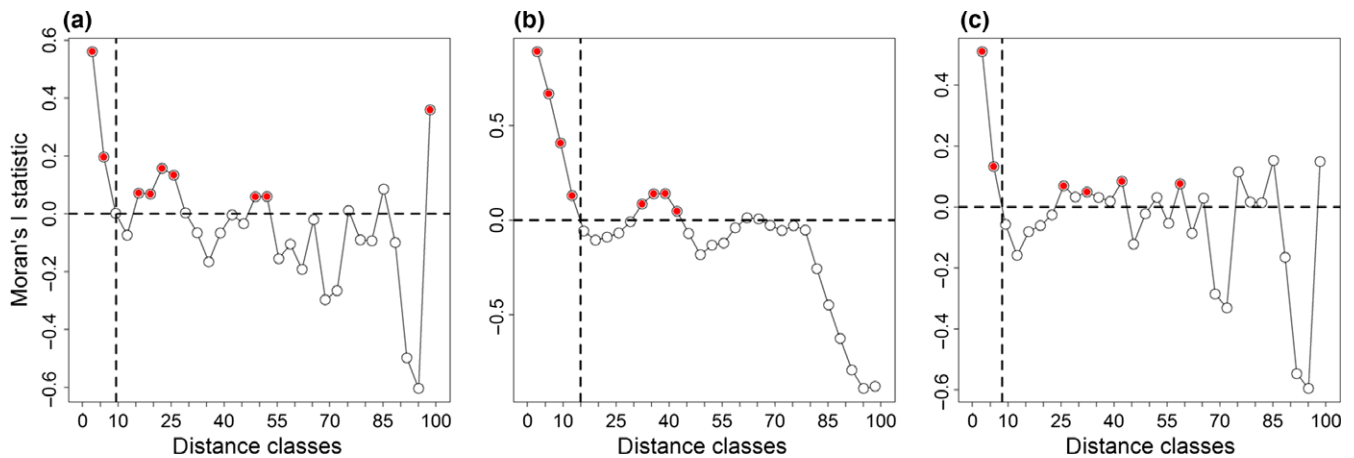


FIGURE 2 Spatial correlograms showing Moran's I as a function of distance classes (metres) at MYI site 06-13 for survey measurements of (a) snow, (b) ice thickness and (c) ice surface topography. Vertical dashed line corresponds to the identified patch size listed in Table 1. Filled red circles are significant values, and open circles are nonsignificant values at $p < .05$

(2014) CryoSat-2 data product and are derived using a modified version of the Warren snow water equivalent climatology (Warren et al., 1999). This included reduction of snow depth over FYI by 50% as suggested by Kurtz and Farrell (2011). Ricker et al. (2014) used sea ice type data (FYI and MYI) from the OSI-SAF daily ice type product as described by Eastwood (2012). All CryoSat-2 data are averaged over an entire month, with data gridded to a 25 by 25 km grid spacing. For the habitat classification, we used the data derived for April 2013 to be closest in time to our sampling period (30 April to 07 May 2013). Ice thickness data are not derived from CryoSat-2 for the months of May through October due to the influence of liquid water within the snowpack on the radar signal. Within the CryoSat-2 data, there were grid cells with missing or unreliable data, which were removed from our analyses. We applied a mask to the CryoSat-2 data as described by Ricker et al. (2014). Data outside this mask were excluded because the snow depth climatology is not valid in these regions (Warren et al., 1999).

We used two different habitat classification systems to classify CryoSat-2 data products into different habitat classes based on ice type, ice thickness and snow depth:

- Hockey stick habitat classification:** Each grid cell is assigned one of five habitat classes based on classification criteria. The two MYI habitat classes were separated based on the mean monthly CryoSat-2 ice thickness. A threshold MYI thickness value of 3.25 m, used to distinguish between the two MYI classes, was determined based on the midpoint between the thickest MYI-Thin site (3.1 m) and the thinnest MYI-Thick site (3.4 m; Table 1). MYI with ice thickness ≥ 3.25 m was classified as 1: MYI-Thick and MYI < 3.25 m was classified as 2: MYI-Thin. FYI was separated into three habitat classes based on the modified Warren monthly climatology snow depth and CryoSat-2 monthly mean ice thickness. FYI with ice thickness < 1.1 m or classified as "new-ice" within CryoSat-2 data was classified as 5: FYI-Young. FYI with ice thickness ≥ 1.1 m and snow depth ≤ 0.17 m was classified as

4: FYI-Thin-snow. FYI with ice thickness ≥ 1.1 m and snow depth > 0.17 m was classified as 3: FYI-Thick-snow. These ice thickness and snow depth classification criteria were applied to the CryoSat-2 data products and assigned the according value of per cent coverage of suitable habitat and the 95% confidence intervals determined from the snow and ice survey-derived T values. All threshold values were determined from *in situ* ice core chl a biomass, and snow and ice survey observations were described in Section 3.2.

- Block-model habitat classification:** Throughout the article, we define the term "block model" as a modelling or up-scaling approach where each grid cell, which is typically of the order of $10s \times 10s$ of kilometres, is assigned one ice thickness and one snow depth value thereby not accounting for spatial variability of these properties within the grid cell. Accordingly, for this habitat classification, a single value of T (Equation 3) was calculated for each grid cell integrated over the ice thickness using k_i (1.55 m^{-1}), snow depth using k_s (20 m^{-1}) and α (0.81, based on the consistent presence of snow). Based on the threshold value of T and the 95% confidence interval (CI_{95}) (see Section 3.2), each grid cell was assigned a habitat class of either suitable ($T \geq \text{threshold}$ and CI_{95}) or not-suitable ($T < \text{threshold}$ and CI_{95}) for ice-algal growth (Table 5).

3 | RESULTS

3.1 | Snow and ice thickness morphology and derived light transmittance

The Lincoln Sea sampling area is a dynamic area due to interaction with, and exchange of, sea ice with the Arctic Ocean. The sampling area was comprised of immobile landfast coastal sea ice at the southern edges and mobile pack ice at its northern extent. The landfast ice consists primarily of consolidated MYI floes with smaller amounts of FYI forming in the interstitial space during freeze-up.

The division between landfast ice and pack ice is not a distinct line but rather a transitional region that can be characterized by ice with limited mobility due to geographic barriers and the intermittent nature of ice export through Nares Strait.

The sampled FYI ice sites can be considered the oldest FYI because the ice formed in the interstitial space between MYI floes during initial freeze-up. FYI surveys had relatively uniform ice thicknesses, with site mean thicknesses in the range 1.6–1.8 m and low intrasite variability (Table 1). Only one sea ice ridge was surveyed at FYI site 03-13 but was only partially surveyed at the end of the transect (Fig. S3). Ice thickness was highly variable between and within MYI sites, with site mean thicknesses ranging between 2.1 and 3.7 m and large intrasite variability (Table 1). Two MYI sites were exceptionally thick with site mean thicknesses of 3.4 m (01-12) and 3.7 m (05-13; Table 1). These two sites were classified as thick MYI ("1: MYI-Thick"; Table 1) and also had the thickest snow cover (>0.4 m; Table 1). The remaining MYI sites were classified as thin MYI ("2: MYI-Thin"; Table 1), and all had comparable median snow depths (0.28 to 0.33 m; Table 1). Snow depth was highly variable within all MYI sites (Table 1). Two FYI sites (02-12 and 03-13) had a significantly (*t*-test, $p < .05$) thicker snow cover with site medians of 0.29 m compared to the other FYI site (02-13) with a median snow depth of 0.17 m (Table 1). The FYI sites were classified into thicker snow ("3: FYI-Thick-Snow") and thinner snow ("4: FYI-Thin-Snow"; Table 1). In general, the snow cover was thicker on MYI (median for all sites 0.34 m) than on FYI (median of all sites 0.25 m); however, the lower range of snow depth observations (25th percentile) was comparable at 0.18 m for FYI and 0.21 m for MYI (Table 1).

The characteristic differences between FYI and MYI observed for all surveys are evident in Figure 3. Based on a visual inspection of the surveys, the level surface morphology and uniform ice thickness from a typical FYI survey (Figure 3a) were obviously different from the undulating surface and highly variable ice thickness from a typical MYI profile (Figure 3b).

One survey was conducted on young FYI (site 05-12), which formed more recently than the older FYI sites by the formation and subsequent refreezing of open water leads. This site consisted of thinner, uniform ice 0.8 m thick and a very thin and uniform snow pack around 0.06 m (Table 1). This site was classified as young FYI ("5: FYI-Young"; Table 1).

Overall, the FYI-Young site had the largest survey-derived *T* (median: 1.8%), with relatively lower variability (Table 1; Figures 4 and 5). The FYI-Thin-Snow site had the second largest survey-derived *T* with an overall median (IQR) of 0.12% (0.04%–0.4%; Table 1; Figures 4 and 5). FYI-Thick-Snow and MYI-Thin sites had comparable survey-derived *T* values with medians (IQR) of 0.0076% (0.002%–0.028%) and 0.0033% (0.0004%–0.029%), respectively (Table 1; Figures 4 and 5). The MYI-Thick sites had the lowest survey-derived *T* values with a median (IQR) of 0.0000% (0.0000%–0.0007%; Table 1; Figures 4 and 5).

ANOVA and post hoc Tukey HSD tests indicated that ice core location *T* values were not significantly different between FYI and MYI-Hum ice types or between FYI-Young and MYI-Hum (Table 2).

However, significant differences in *T* were observed for all other combinations of ice types (Table 2; Figure 6). FYI-Young cores had the highest *T*, and MYI-RP had the lowest *T* values (Figure 6b). MYI-Hum and FYI core *T* values were in between FYI-Young and MYI-RP *T* values. MYI-Hum ice core *T* values were generally more uniform than FYI *T* values (Figure 6b) but with overlapping ranges of values.

The snow depth, sea ice thickness and surface topography transects conducted in 2013 are shown in the supplementary material (Figs S1–S8). The directional comparison, west–east vs. south–north, of the eight perpendicular snow and ice surveys showed significant differences for ice thickness at four sites, for snow depth at five sites and for ice freeboard at three sites (Table 3).

From the snow and ice survey data, we found significant ($p < .05$) negative correlations between snow depth and ice freeboard for the FYI-Young site ($r = -.56$), FYI sites ($r = -.69$) and MYI sites ($r = -.73$; Table 4). All other correlations were not significant (Table 4).

Spatial autocorrelation analyses using spatial correlograms indicated larger sea ice thickness patch sizes (P_i) for FYI (~30 m) than for MYI (14–24 m; Table 1). Snow patch sizes (P_s) were generally larger for FYI (30–45 m) compared to MYI (9–25 m; Table 1). Freeboard (surface topography) patch sizes (P_{fb}) were also typically larger for FYI (25–39 m) than MYI (6–25 m); however, two MYI sites (01-13 and 04-13) had patch sizes comparable to FYI (23–25 m; Table 1). The other four MYI sites had surface topography patch sizes between 6 and 10 m (Table 1). Patch sizes for each variable and site are summarized in Table 1, and spatial correlograms for each site and variable are shown in supplementary material (Figs S9–S16).

3.2 | Chl *a* biomass

ANOVA and post hoc Tukey HSD tests indicated that ice core chl *a* biomass was significantly higher in MYI-Hum ice cores than FYI and MYI-RP ice cores ($p < .05$; Table 2 and Figure 6a). No significant differences in ice core chl *a* biomass were observed between the other ice types (Table 2 and Figure 6a). Three bottom-ice cores (triplicates) were taken from the same hummock at site 06-13; the mean of the triplicate core sections, 2.53 mg/m², was the maximum value used in the ANOVA and Tukey tests (Figure 7). Two of the triplicate cores had the highest (3.59 mg/m²) and second highest (2.73 mg/m²) biomass values of all cores (Figure 7). The third triplicate had the sixth highest biomass (1.26 mg/m²). The three other MYI hummocks sampled were among the top eight highest biomass of all bottom-ice cores (Figure 7).

Two anomalous ice cores were identified as follows: core 06-13-RP had anomalously high chl *a* biomass (0.55 mg chl *a* m⁻²) given its low calculated *T* value (0.00008%). Station 06-13-RP was one of two snow removal sites (this one was ~5 m away from the edge of the sampled hummock). Therefore, we had under-ice PAR measurements (data not presented here) that were ~500 times greater than expected based on the thick snow cover (~0.4 m), which was likely due to horizontal light scattering from the nearby hummock (see

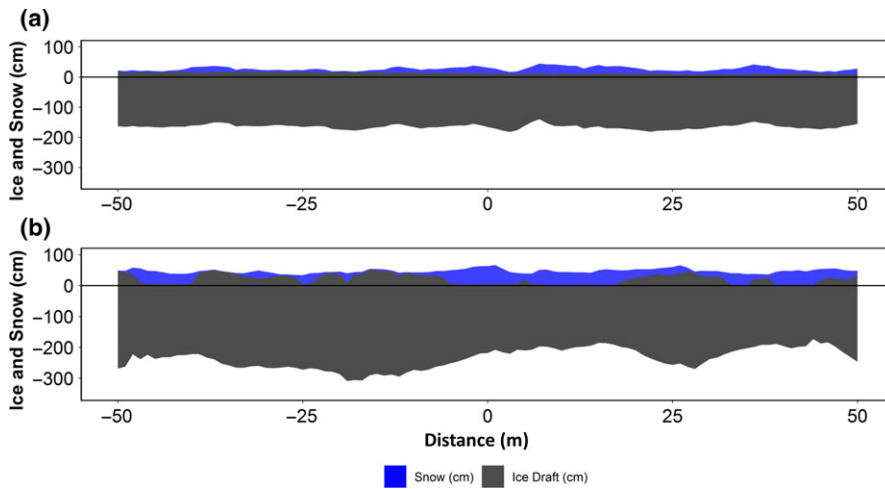


FIGURE 3 Snow and sea ice surveys conducted at a) FYI site O2-12 showing the south-north transect and b) MYI site O6-13 showing the West-East transect

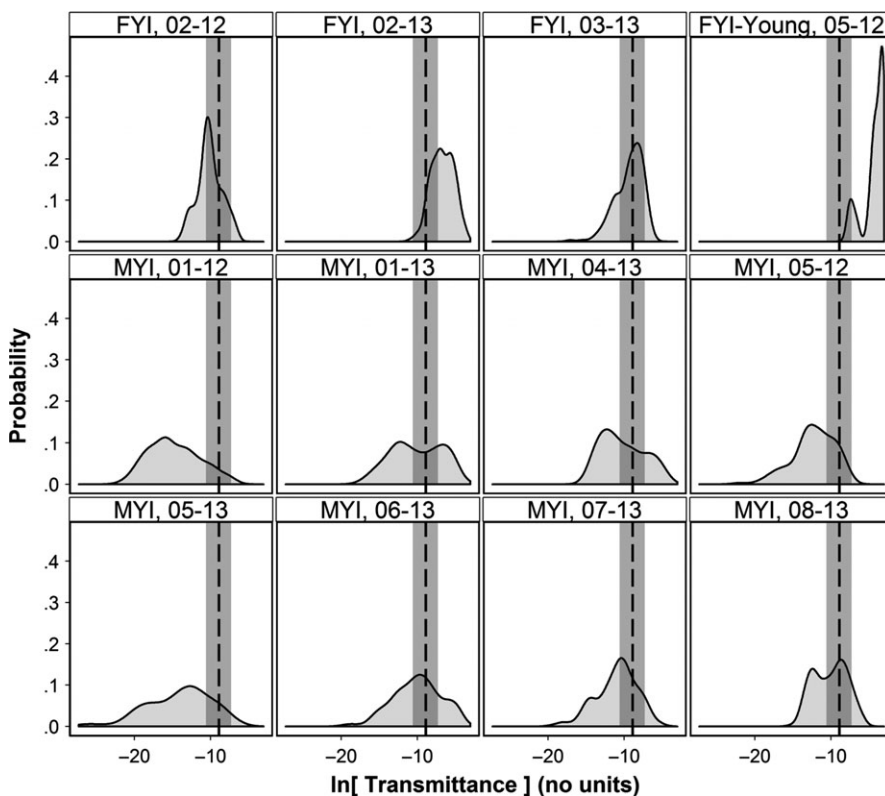


FIGURE 4 Probability density distributions of log-transformed transmittance calculated from the snow and sea ice surveys for each site. Dashed vertical line corresponds to the threshold transmittance value of 0.014% (log space = -8.9). Grey shaded area represents the 95% confidence interval

Section 4.2). Core O6-12 had anomalously low chl *a* biomass ($0.05 \text{ mg chl } a \text{ m}^{-2}$) given its high *T* value (4.1%). Core O6-12 was removed from the piecewise hockey stick regression analysis. Furthermore, the second FYI-Young core was also removed from the hockey stick regression analysis due to the drastically different morphological history of FYI-Young ice compared to the older FYI and MYI (e.g., ice growth rates and the influence on establishing ice-algal communities). This is discussed in more detail in Section 4.2.

Overall, phaeopigment concentrations were, on average, 0.18 mg/m^3 . Chl *a* represented, on average, $67.3\% \pm 15.4\%$ of the total pigments for all core sections analysed.

Hockey stick regression analysis between chl *a* biomass and *T* separated the ice core data into two distinct groups (Figure 7): (i) suitable habitat for ice-algal growth indicated by relatively higher chl

a biomass ($>0.5 \text{ mg chl } a \text{ m}^{-2}$) and (ii) not-suitable habitat for algal growth indicated by near-zero chl *a* biomass ($<0.5 \text{ mg chl } a \text{ m}^{-2}$) and a regression line with a slope of approximately zero. The threshold *T* value determined from the hockey stick regression analysis was $T = 0.014\%$ with a 95% confidence interval between 0.0025% and 0.068% (Figure 7).

3.3 | Floe-scale spatial coverage of suitable sea ice-algal habitats

Based on the determined *T* threshold value of 0.014%, we identified the spatial coverage along each snow and ice survey with $T \geq 0.014\%$ and classified these regions as suitable habitat for ice-algal growth. The per cent coverage of suitable ice-algal habitat for

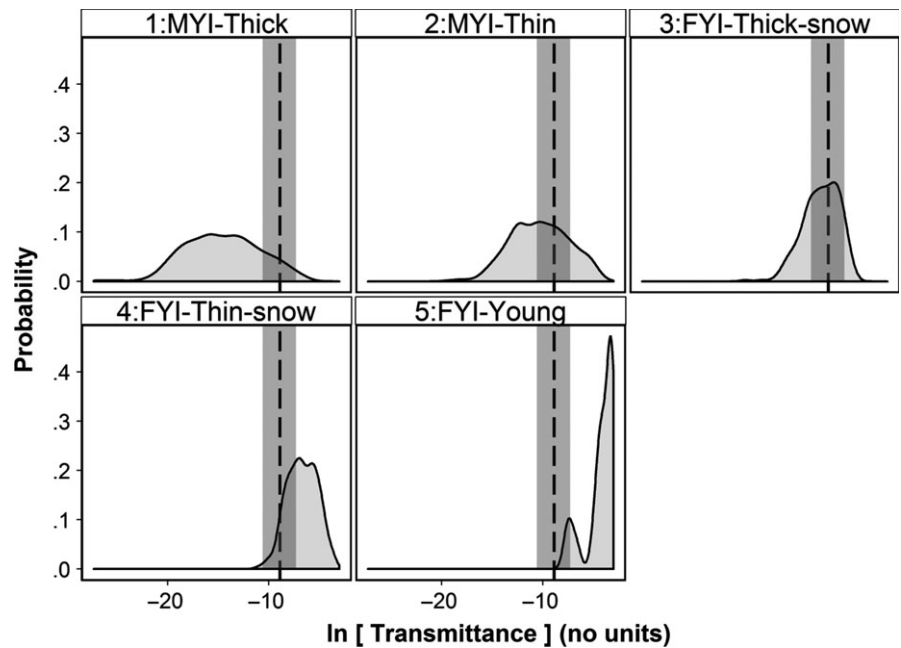


FIGURE 5 Probability density distributions of log-transformed transmittance calculated from the snow and sea ice surveys combined for each ice class. Dashed vertical lines corresponds to the threshold transmittance value of 0.014% (log space = -8.9). Grey shaded area represents the 95% confidence interval

TABLE 2 Post hoc Tukey HSD test results showing the adjusted *p*-value matrix for multiple comparison of the means of the log-transformed chl *a* biomass and corresponding calculated transmittance (*T*) between the different ice types at ice core locations

Variable	Ice type	FYI	FYI-Young	MYI-RP	MYI-Hum
Chl <i>a</i>	FYI (N = 6)	–			
	FYI-Young (N = 2)	0.87	–		
	MYI-RP (N = 13)	0.986	0.74	–	
	MYI-Hum (N = 4)	0.047	0.52	0.013	–
<i>T</i>	FYI (N = 6)	–			
	FYI-Young (N = 2)	0.01	–		
	MYI-RP (N = 13)	0.009	0.000	–	
	MYI-Hum (N = 4)	0.24	0.30	0.0001	–

Bold values indicate significant difference between ice types ($p < .05$).

all ice types showed a significant relationship with site median snow depth ($R^2 = 0.82$). The FYI-Young class had the highest coverage of suitable habitat at 100% (CI₉₅: 93%–100%); second highest was the FYI-Thin-snow class at 94% (CI₉₅: 65%–100%; Table 1). FYI-Thick-snow and MYI-Thin classes had comparable suitable ice-algal habitat coverage at 40% (CI₉₅: 8%–71%) and 33% (CI₉₅: 17–54; Table 1), respectively, although FYI-Thick-snow had larger uncertainty. The MYI-Thick class had the lowest suitable habitat coverage of 7% (CI₉₅: 2–16; Table 1). Station 05-12 was not included in the habitat classes because we had low confidence that the survey representatively sampled the ice types of the floe due to the short survey length and the fact it was only in one direction.

3.4 | Pan-Arctic-scale spatial coverage of suitable sea ice-algal habitats

Excluding missing data and grid cells outside the data mask (Figure 8), MYI had a total area of 1.83×10^6 km² (28% of total ice area), FYI had a total area of 4.30×10^6 km² (67%), and FYI-Young ice had a total area of 0.31×10^6 km² (4.7%; Table 5). Class 4: FYI-Thin-snow had the largest areal coverage of suitable habitat with 2.81 million km² representing ~44% of the total ice area (Table 5). The areal coverage of suitable habitat for class 5: FYI-Young was 0.31 million km² representing 4.7% of total ice area (Table 5). Habitat classes 2: MYI-Thin and 3: FYI-Thick-Snow had the same areal coverage of 0.53 million km² representing 8.2% of the total ice area (Table 5). Class 1: MYI-Thick had the lowest areal coverage of suitable habitat of 0.02 million km² representing only 0.3% of the total ice area (Table 5).

Based on the block-model habitat classification, MYI contributed substantially less to the overall suitable habitat coverage compared to the observation-based approach (Figure 8 and Table 5). It is apparent from Figure 8d that a large majority of the MYI cover is classified as not-suitable for ice-algal growth, with an estimated suitable MYI-algal habitat area of only 0.02 million km² representing 0.3% of the total ice area (Table 5). This is over an order of magnitude less suitable MYI-algal habitat coverage compared to the hockey stick classification of MYI habitat (Table 5). On the other hand, suitable habitat coverage for FYI was similar using both classification systems with the block model showing suitable habitat coverage for FYI of around 4 million km² and the hockey stick classification for FYI was 3.3 million km² (Table 5).

The range of uncertainty values for MYI habitat classes have a more uniform spread relative to the overall suitable habitat coverage estimate in comparison with FYI for both classification systems. This is evident from the upper and lower limits of the CI₉₅ for suitable

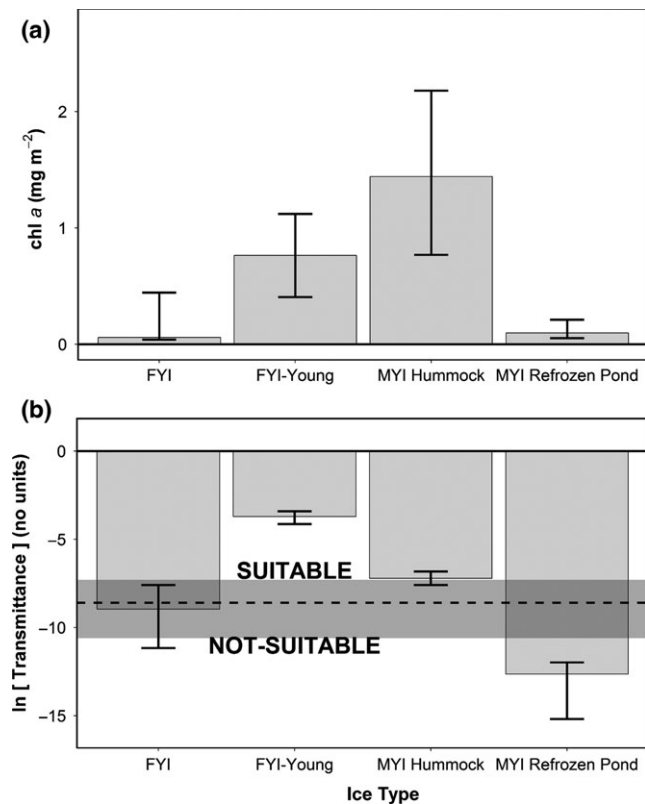


FIGURE 6 Comparison between ice types from ice core data: (a) chl *a* biomass and (b) log-transformed calculated transmittance (T). Bars represent the median, and error bars the interquartile range (25th and 75th percentiles). Dashed horizontal line in (b) is the threshold $T = 0.014\%$ (log space = -8.6). Horizontal grey shaded area in (b) represents the 95% confidence interval for the threshold T value

MYI-algal habitat, which had comparable absolute differences to the overall estimate for both classification systems. FYI on the other hand had lower limits of the CI_{95} with much greater absolute differences relative to the overall estimate in comparison with the upper limits of the CI_{95} (Table 5 and Figure 8). This suggests a potential bias for estimating suitable FYI-algal habitat.

4 | DISCUSSION

4.1 | Sea ice-algal chl *a* biomass in different ice types

To the best of our knowledge, the bottom-ice biomass values from MYI hummock ice (range $0.62\text{--}3.6$ mg chl *a* m⁻²; $4.1\text{--}35.9$ mg chl *a* m⁻³; Figure 6a) are among the highest reported from Arctic springtime MYI. Melnikov, Kolosova, Welch, and Zhitina (2002) observed comparable maximum bottom-ice-algal chl *a* concentrations of 9.32 mg/m³ in MYI from the Beaufort/Chukchi Seas during July. Schünemann and Werner (2005) reported MYI bottom chl *a* concentration of 3.4 mg/m³ during late-winter (April) in Fram Strait. Lange et al. (2015) argued in combination with the Schünemann and Werner (2005) study that high bottom-ice-algal biomass may be common

features associated with MYI hummocks due to their typically thinner or absent snow cover resulting in more available light for bottom-ice algae. Based on a more representative sample size, this study provides evidence that MYI hummocks can support sea ice chl *a* biomass in the upper range of values reported for MYI in the Arctic Ocean (Melnikov et al., 2002; Schünemann & Werner, 2005) and higher than those observed in FYI in the same region. These results reinforce the hypothesis proposed by Lange et al. (2015) that MYI hummocks are a suitable habitat for sea ice-algal biomass, which can be attributed to more available light due to a typically thinner or absent snow pack compared to the surrounding MYI with a more uniform surface topography.

Of the two FYI-Young cores sampled in this study, one core had high chl *a* biomass comparable to the MYI-Hum cores, which we can also attribute to high bottom-ice light levels due to a thin, uniform snow pack and thin ice. The other FYI-Young core had the thinnest snow cover and thinnest sea ice of any cores considered in this study. However, it had near-zero chl *a* even though light levels within the bottom-ice layer would have been high. Lange et al. (2015) attributed the low biomass to either light levels that were too high and inhibited algal biomass growth and accumulation (Barlow et al., 1988; Juhl & Krembs, 2010; Michel, Legendre, Demers, & Therriault, 1988), or sea ice growth rates were too rapid and there was not sufficient time (i.e., due to recent formation of the ice) to establish substantial algal biomass (Legendre, Aota, Shirasawa, Martineau, & Ishikawa, 1991). Regardless of the higher light levels present under FYI-Young ice types, higher chl *a* biomass was observed in three of the bottom-ice hummock samples. This confirms the premise that something other than available light is limiting algal growth, which is contrary to the assumption of the habitat classification. Therefore, we excluded the FYI-Young cores from the hockey stick regression analysis. Nevertheless, in the habitat classification analysis, we did assign FYI-Young ice as having 100% suitable habitat coverage, which we must note is solely based on the available light for bottom-ice-algal communities but does not account for the potentially different environmental histories of this ice type. We suggest further work is required to determine a maximum T threshold value to be considered in future habitat mapping studies.

One potential explanation for the lower than expected chl *a* biomass from FYI sites with high potential light availability is that the snow cover is continuously being redistributed, which would result in a continuously changing light regime for the ice-algal communities at the bottom of FYI. This is a consequence of the level surface topography typical of FYI, which is apparent from the snow and ice survey at FYI site O2-12 (Figure 3a). This results in a drifted snow pack that is redistributed based on wind speed and direction and is continuously changing as there are no surface ice features (e.g., ridges or hummocks) that can “trap” the snow (note: we are only referring to level FYI). Therefore, constant changes in the FYI snow cover may have resulted in a thicker snow pack averaged over a longer period immediately before our measurements, in effect diminishing the capacity for FYI to accumulate chl *a* biomass compared to MYI hummocks. The snow pack could have also been thinner.

TABLE 3 Directional comparison of snow and sea ice surveys from 2013 summarized by west–east (WE) and south–north (SN) transect directions

Site	Ice Type	Mean h_i (m) ^a		Median (IQR) h_i (m) ^a		Median (IQR) h_s (m) ^a		Median (IQR) fb (m) ^a		rms _{fb}	
		WE	SN	WE	SN	WE	SN	WE	SN	WE	SN
02-13	FYI	1.7	1.8	1.7 (1.6–1.7)	1.8 (1.7–1.8)	0.20 (0.15–0.25)	0.13 (0.08–0.19)	0.11 (0.10–0.12)	0.12 (0.10–0.16)	0.11	0.13
03-13	FYI	1.6	1.6	1.6 (1.6–1.7)	1.6 (1.5–1.7)	0.28 (0.24–0.34)	0.31 (0.25–0.40)	0.05 (0.03–0.07)	0.04 (0.01–0.07)	0.06	0.06
01-13	MYI	2.7	3.1	2.7 (2.1–3.2)	2.8 (2.2–3.9)	0.36 (0.15–0.47)	0.28 (0.04–0.41)	0.11 (0.04–0.31)	0.18 (0.02–0.45)	0.22	0.34
04-13	MYI	3.4	2.7	3.3 (2.8–4.0)	2.7 (2.2–3.2)	0.32 (0.17–0.42)	0.34 (0.1–0.45)	0.16 (–0.03 to 0.37)	11.5 (–0.03 to 0.33)	0.28	0.27
05-13	MYI	3.7	3.7	3.2 (3.0–4.1)	3.6 (3.2–4.3)	0.44 (0.31–0.68)	0.41 (0.22–0.6)	0.22 (0.0–0.36)	0.33 (0.16–0.48)	0.30	0.40
06-13	MYI	2.6	2.9	2.5 (2.1–2.9)	3.2 (2.5–3.3)	0.26 (0.1–0.43)	0.28 (0.2–0.42)	0.22 (0.04–0.35)	0.23 (0.15–0.34)	0.26	0.27
07-13	MYI	2.6	2.5	2.6 (2.4–2.8)	2.5 (2.1–2.8)	0.28 (0.21–0.35)	0.4 (0.31–0.53)	0.25 (0.16–0.32)	0.17 (0.07–0.27)	0.22	0.31
08-13	MYI	2.1	2.1	1.9 (1.7–2.5)	2.0 (1.8–2.5)	0.35 (0.27–0.42)	0.27 (0.21–0.43)	0.8 (0.05–0.14)	0.13 (0.06–0.19)	0.15	0.19

“rms” refers to the root-mean-square.

^aBold values correspond to significant differences ($p < .05$) and italics correspond to differences with $0.05 < p < .1$, based on t tests comparing the WE and NS perpendicular transects.

TABLE 4 Correlation matrix between the snow and ice survey-derived properties: snow depth (h_s), ice thickness (h_i), ice freeboard (fb) and log-transformed calculated transmittance (T)

Ice type	Variable	h_s	fb	h_i
Lead ice	h_s	–		
	fb	–0.56*	–	
	h_i	–0.13	0.34*	–
	$\ln[T]$	–0.99*	0.57*	0.11
FYI	h_s	–		
	fb	–0.69*	–	
	h_i	–0.37*	0.57*	–
	$\ln[T]$	–0.97*	0.56*	0.21*
MYI	h_s	–		
	fb	–0.73*	–	
	h_i	–0.27*	0.66*	–
	$\ln[T]$	–0.92*	0.50*	–0.06*

*Indicates significant correlations ($p < .05$), and bold indicates strong correlations ($r \geq .5$).

However, if this were the case, we would have expected to observe higher biomass. Furthermore, if the snow pack was indeed thinner before our sampling, then this would strengthen our premise that the continuously changing snow pack has a negative impact on ice-algal growth even under suitable light conditions. Ice algae that stops and starts growing under continuously changing light conditions would be far less efficient than ice algae with more consistent growth conditions, for example MYI hummocks with consistently low-snow cover. This is because photoadaptation involves breakdown and synthesis of biomolecules (e.g., pigments and enzymes), which has an energy cost and a delayed response on the order of days (Michel et al., 1988).

Observed differences in chl *a* do not necessarily translate into differences in carbon biomass due to lower C:chl *a* ratios in low light

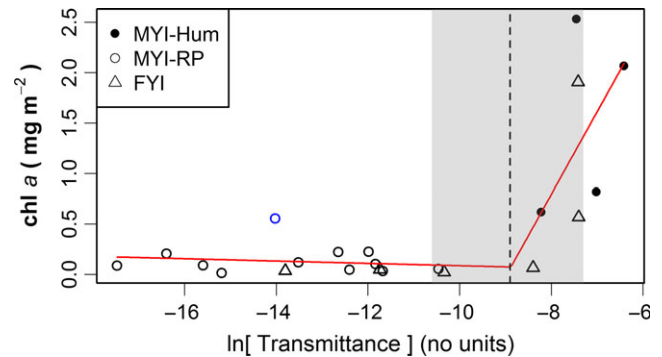


FIGURE 7 Piecewise “hockey stick” regression analysis plot. Red solid line segments are the two fitted piecewise regressions. Dashed vertical line indicates the threshold value (aka: change point) of the natural log-transmittance identified by the regression analysis. Grey shaded area indicates the 95% confidence interval for the threshold value. Blue open circle corresponds to core 06-13-RP located adjacent (~5 m) to a hummock

environments compared to high light environments (e.g., Michel et al., 1988) and the likely contribution of nonalgal carbon within ice communities. Therefore, the chl *a* biomass distinction can confidently help identify distinct regimes of suitable vs. unsuitable ice-algal habitat in terms of available light. Interpreting the variability in chl *a* biomass within those ice-algal habitat classes, however, would require additional physiological and biogeochemical data.

4.2 | In situ survey-based sea ice-algal habitat classification

Using piecewise “hockey stick” regression is an established approach to identify ecological thresholds (e.g., Toms & Lesperance, 2003; Toms & Villard, 2015). Our application of hockey stick regression indicated a reliable threshold value for transmittance (T), with associated confidence intervals (CI_{95}) needed to address the potential

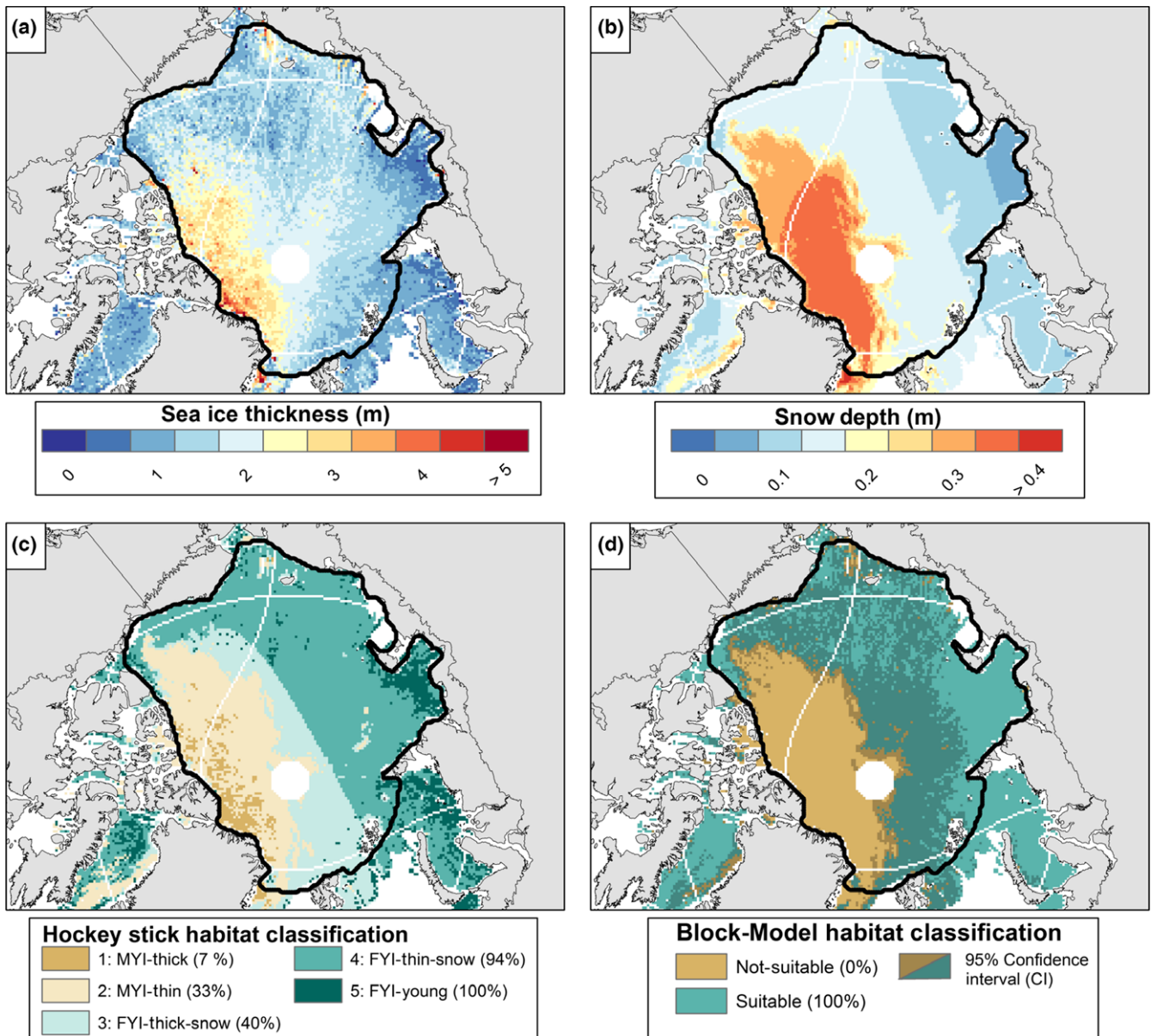


FIGURE 8 Maps of the Arctic Ocean showing: (a) CryoSat-2 derived sea ice thickness for April 2013 (Ricker et al., 2014), (b) snow depth for April 2013 based on the modified Warren snow climatology (Warren et al., 1999) and (c) hockey stick habitat classification criteria applied to sea ice thickness and snow depth from a) and b); and d) block-model habitat classification applied to sea ice thickness and snow depth from a) and b). Percentages shown in parentheses represent the per cent coverage of suitable habitat for the corresponding habitat class. Only sea ice thickness and snow depth data within the “Mask” (delineated by the thick black line) were used in our analyses, as the data outside this regions are not reliable (Ricker et al., 2014). CryoSat-2 data products were acquired from www.meereisportal.de

uncertainty of this approach. The threshold T value and CI_{95} was applied to the T values calculated for our snow and ice survey as the first step of the hockey stick habitat classification system.

Taking a block-model habitat classification approach using the survey median values for habitat classes 4: FYI-Thin and 5: FYI-Young would result in 100% suitable ice-algal habitat coverage, which is similar to what was determined taking into account the spatial variability of the entire surveys (Table 1). The CI_{95} for the FYI-Thin-Snow surveys, however, had a large range indicating that assigning only one value to this ice type is not an appropriate approach. On the other hand, FYI-Young ice had CI_{95} between 93

and 100%, suggesting that this ice type may be classified as 100% suitable ice-algal habitat with high confidence.

The habitat classes with thick snow packs (FYI-Thick-Snow, MYI-Thin and MYI-Thick) would all be classified as 0% suitable ice-algal habitat using the block-model approach, whereas the actual observed coverage of suitable habitat was between 7 and 40% and upper ranges of the CI_{95} between 16 and 71% (Table 1). Iacozza and Barber (1999) showed a similar assessment of different ice types in terms of light transmittance and determined that accounting for the spatial variability of snow depth is crucial due to the nonlinear relationship between light transmittance and snow depth. This means

TABLE 5 Summary of the pan-Arctic suitable ice algae habitat area derived by applying the “hockey stick regression” and “block model” classification approaches to the April 2013 CryoSat-2 ice thickness and snow depth data

Classification approach	Habitat class/ Ice type	Class criteria	% suitable habitat per ice class/ type (CI)	Areal coverage per ice class/type [10 ⁶ km ²]	Areal coverage of suitable habitat [10 ⁶ km ²] (CI)	Per cent suitable habitat of total ice area % (CI)
Hockey stick	1:MYI-thick	MYI ≥ 3.25 m	7 (2–16)	0.45	0.02 (0.00–0.04)	0.3 (0.1–0.6)
	2:MYI-thin	MYI < 3.25 m	33 (17–54)	1.39	0.53 (0.27–0.87)	8.2 (4.2–13.4)
	3:FYI-thick-snow	FYI ≥ 1.1 m and snow ≥ 0.17	40 (8–71)	1.31	0.53 (0.11–0.93)	8.2 (1.6–14.5)
	4:FYI-thin-snow	FYI ≥ 1.1 m and snow < 0.17	94 (65–100)	2.99	2.81 (1.94–2.99)	43.6 (30.1–46.4)
	5:FYI-Young	Ice < 1.1 m	100 (93–100)	0.31	0.31 (0.28–0.31)	4.7 (4.4–4.7)
	MYI		30 (15–51)	1.83	0.54 (0.28–0.90)	8.5 (4.3–14)
	FYI		78 (48–91)	4.30	3.3 (2.1–3.9)	52 (32–60)
	FYI-young		100 (93–100)	0.31	0.31 (0.28–0.31)	4.7 (4.4–4.7)
	Total		65 (40–80)	6.44	4.2 (2.6–5.1)	65 (40–80)
Classification approach	Habitat class/ Ice type	Class criteria	% suitable habitat per ice class/type (CI)	Areal coverage per ice class/type [10 ⁶ km ²] (CI)	–	Per cent of total ice area % (CI)
Block model	1: Not-Suitable Algae Habitat	T > 0.014 (CI) %	0%			
	MYI			1.81 (1.68–1.83)		28.2 (26.1–28.5)
	FYI			0.31 (0.02–2.98)		4.9 (0.38–46.3)
	FYI-Young			0.00 (0.00–0.004)		0.00 (0.00–0.07)
	Total			2.1 (1.7–4.8)		33.1 (26.5–74.8)
	2: Suitable Algae Habitat	T < 0.014 (CI) %	100%			
	MYI			0.02 (0.00–0.15)		0.31 (0.00–2.4)
	FYI			3.99 (1.32–4.28)		61.9 (20.5–66.4)
	FYI-Young			0.30 (0.30–0.30)		4.7 (4.6–4.7)
	Total			4.3 (1.6–4.7)		66.9 (25.2–73.5)

that site-summarized snow depths (e.g., mean or median values) are not appropriate to assess the influence of the overall snow pack on light transmittance (Iacozza & Barber, 1999). Together with our results, this emphasizes that block-model classification systems or modelling applications of sea ice algae growth and primary production (Dunne et al., 2012; Dupont, 2012; Vancoppenolle, Meiners et al., 2013) have a high probability of underestimating the potential of ice-algal habitats, which is largely due to the spatial variability of snow on the different sea ice types.

Spatial heterogeneity of sea ice-algal biomass is related to the distribution of snow on FYI during spring, due to the large influence of snow on light transmission, with snow patch sizes reported between 10 and 90 m (Gosselin et al., 1986; Mundy, Barber, & Michel, 2005). Similarly, our spatial autocorrelation analyses demonstrated snow patch sizes, P_s, between 30 and 45 m for snow on FYI. Our results also showed that the variability of suitable habitat on FYI was largely controlled by the snow pack, which is spatially redistributed by wind creating the wave-like snow drifts with peaks (high snow) and troughs (low snow). Gosselin et al. (1986) suggested

wind-induced drifting resulted in short-term variability of the snow pack, which also influenced the distribution and perhaps redistribution or recolonization of bottom-ice-algal communities. This supports our proposition that FYI-algal biomass growth and accumulation may be limited based on the short-term temporal variability of the snow pack and hence available light for bottom-ice-algal communities.

Snow distribution also had a large influence on the spatial coverage of suitable ice-algal habitat for MYI. There were distinct differences, however, between FYI and MYI as a result of the different mechanisms and features controlling the distribution of snow on MYI. Contrary to FYI, which has a snow pack in a continuous state of change due to wind-driven redistribution, the snow distribution on MYI is strongly influenced by the highly undulating ice surface topography where snow accumulates in topographic lows or regions adjacent to hummocks and is removed or has substantially less accumulation on the surface of hummocks (Iacozza & Barber, 1999; Perovich et al., 2003; Sturm et al., 2002). This relationship between snow and ice surface is apparent from the MYI snow and ice survey (Figure 3b) and was a consistent feature observed at all MYI sites

(Figs S1, S4–S8). Spatial autocorrelation analyses for MYI sites showed surface topography patch sizes mostly between 6 and 10 m; however, ~25 m patches were observed at two sites. The surface topography patch sizes were interpreted as the size of hummocks. The 6–10 m hummock size range was obvious from the snow and ice surveys and was the most obvious size range for the undulating surface features in all surveys with only a few larger hummocks ~25 m (Figure 3b and Figs S1–S16). The observed distribution of snow in relation to the highly undulating MYI surface indicates that the horizontal variability of snow on MYI is also a relatively constant feature with more snow at low points (e.g., refrozen melt ponds) and adjacent to hummocks (or ridges) but no or little snow accumulation on hummocks. This is an important distinction from FYI, as MYI hummocks represent a constant low-snow environment, which are not subject to rapid changes in snow depth and bottom-ice light availability, and thus can be considered a more stable habitat for sea ice algae.

The quantification of typical MYI hummock sizes and FYI snow drift sizes also has important implications for airborne and satellite remote sensing of snow and subsequently the potential for developing sea ice-algal habitat classification systems from such large-scale pan-Arctic observations. The common size range of snow-free/low-snow hummocks between 6 and 10 m suggests that airborne or satellite sensors would need to have at least the same spatial resolution in order to capture the variability of the snow on these features. This is also the case for FYI with our observed snow drifts ranging between 30 and 45 m and other studies between 10 and 90 m (e.g., Gosselin et al., 1986; Iacozza & Barber, 1999; Mundy et al., 2005). Therefore, in order to observe the multiscale variability (e.g., floe scale, regional, pan-Arctic) of snow on MYI and FYI, without the current requirement of extensive ground surveys, there is a need for improved satellite and airborne sensors that can resolve these spatial scales. At present, even the best airborne snow radar measurements have too coarse of a spatial resolution and large uncertainties to be useful for characterizing the spatial variability of snow depths at the required scale, and further improvements in snow depth observations are needed (Kurtz & Farrell, 2011; Kwok & Haas, 2015; Newman et al., 2014).

Suitable sea ice-algal habitat for MYI had high variability between sites, which was related to overall mean site ice thickness. MYI-Thick sites (mean ice thickness >3.25 m) had substantially less suitable habitat than MYI-Thin sites, which was the result of thicker hummock ice with T values smaller than the threshold value. Under snow-free conditions, a T value of 0.014% corresponds to an ice thickness of ~5 m. This means that MYI sites with mean ice thicknesses >3.25 m had a high proportional coverage of hummocks thicker than ~5 m, which did not represent suitable ice-algal habitat even under snow-free conditions.

One exception to this pattern was site 05-12 (Table 1), which was conducted in only one direction and covered a shorter survey length (130 m) than the others sites. Comparison between the perpendicular west–east and south–north surveys at each site indicated significant differences between all physical parameters at most sites, suggesting site 05-12 may not be representative of the surveyed ice floe. Gosselin et al. (1986) also showed that the orientation of

survey transects was critical in identifying the spatial variability of snow on FYI and the resulting influence on the spatial distribution of bottom-ice-algal biomass. On level FYI, snow drift patterns are wave-like undulations of snow depth with uniform snow features (e.g., snow drifts or valleys) forming perpendicular to the wind direction. Therefore, it is possible to conduct single linear surveys oriented parallel to a snow drift that do not cross the snow drift. On MYI, the snow (re-) distribution pattern is less likely to have a similar influence on the representativeness of the sampling because the ice surface topography primarily controls snow distribution. Though hummocks may not have a direct relationship to wind direction, it would still be possible to survey a single profile line, which predominantly covers the “valley” between hummocks and does not representatively capture the undulating surface topography and snow distribution on MYI. This sampling bias is eliminated or significantly minimized when conducting perpendicular survey transects. A single direction survey was conducted for FYI-Young ice; however, due to the typical uniform distribution of snow and ice on this ice type, perpendicular transects are not necessary to capture this small variability.

For MYI, we demonstrated a reliable observation-based habitat classification system, which was possible due to the relatively stable pattern of snow distribution on MYI (thin-snow on hummocks, thick snow on refrozen ponds), which was independent of median snow depth. This also implies that upscaling such a habitat classification system to larger-scale satellite or airborne remote sensing observations would be more robust for MYI. This is due to the fact that observation systems and modelling of sea ice thickness are much more reliable and established than observations and forecasts of snow depth on sea ice (Kurtz & Farrell, 2011; Kwok & Haas, 2015; Newman et al., 2014). Modelling a relatively static system, such as the distribution of hummocks, can be assumed to be more reliable than a dynamic system, such as wind-driven snow distribution.

We surveyed fewer FYI sites and observed high variability in snow depth at the surveyed sites. With no constant sea ice surface features on FYI, the snow surface and suitable habitat can vary on short time scales in an unpredictable manner. Nonetheless, we did observe a relationship between suitable habitat coverage and median snow depth. Using these criteria, we were able to classify FYI into two classes based on the amount of snow accumulation. However, there remains a strong need for more ground-truthing of snow depths on FYI in order to assess the reliability of applying the habitat classification to larger scales.

4.3 | Pan-Arctic habitat classification

Overall, MYI accounted for nearly one-third of the total ice area, with an associated suitable habitat coverage corresponding to 8.5% of the total ice area. Accounting for the variability of the MYI snow and ice properties using the hockey stick habitat classification system resulted in suitable habitat coverage estimates 27 times greater than the block-model-based approach. These findings indicate MYI is an overlooked region in terms of potential for ice-algal growth,

which likely has a significant and underestimated contribution to the total algal biomass and carbon budget of the Arctic Ocean.

We must also consider that these estimates for hummocks are likely an underestimate due to the potential influence of horizontal light scattering around hummocks, which we observed to extend to a distance of ~5 m from the hummock edge. This emphasizes that suitable habitat around hummocks is even greater than we have shown. The potential implications of horizontal light scattering around hummocks require further investigation in order to quantify these regions.

Suitable FYI habitat largely comes from the thin-snow FYI class, which indicates that snow depth over FYI is of high importance. This means the accuracy of suitable habitat estimates for FYI is highly dependent on the accuracy of the snow depth measurements, which are currently derived from the modified Warren climatology.

The application of this habitat classification does not account for the presence of sea ice ridges, which can make-up a substantial portion of the overall ice pack (Haas, Hendricks, Eicken, & Herber, 2010). Since we did not conduct snow and ice surveys or sea ice coring on ridged ice, we cannot include these features in our analyses. When travelling on sea ice, it is common to see ridged sea ice regions with large, vertical snow-free ice chunks. Snow-free ridges and hummocks have been previously document from other studies (Iacozza & Barber, 1999; Perovich et al., 2003; Sturm et al., 2002). Therefore, we could also speculate that light transmittance under snow-free ridges may also produce a suitable habitat in much the same way hummocks are considered a suitable habitat. Based on this premise, our habitat classification would be an underestimate of the suitable habitat for both ice types. The study of sea ice ridges is logistically demanding, even more so than 4 m hummock ice. Nevertheless, we strongly recommend physical and biological sampling of sea ice ridges in order to assess the potential of sea ice ridges as another overlooked region of suitable ice-algal habitat, which could become even more important as MYI continues to decline.

4.4 | Implications of MYI loss

Most of the thick MYI with low suitable habitat coverage is in the region north of the Canadian Arctic Archipelago and Greenland where the thickest sea ice in the Arctic is located (Haas, Hendricks, & Doble, 2006; Haas et al., 2010). Submarine sonar ice thickness measurements conducted during the period 1958–1976 had mean ice thicknesses well over 3 m in all regions of the Arctic Ocean except the Beaufort and Chukchi Seas. Basinwide Arctic sea ice thickness observations during winter 1980 had a mean of 3.64 m (Kwok & Rothrock, 2009). Since the early 1990s mean ice thicknesses for all regions have been well below 3.25 m (Kwok & Rothrock, 2009). Based on our established MYI thickness threshold of 3.25 m, we speculate that this shift from thick MYI, which dominated the Arctic Ocean up until the 1980s, to thin MYI in the 1990s was accompanied by an increase in the suitable ice-algal habitat coverage.

As MYI continues to thin and be replaced by FYI, our findings suggest that the spatial coverage of suitable ice-algal habitat will largely depend on the temporal and spatial distribution of snow on sea

ice, which will be influenced by continued warming of the Arctic ocean and atmosphere. Our findings for FYI suggest that with projections for an overall increase in snow precipitation (IPCC, 2013), there would be similar or decreased spatial coverage of suitable ice-algal habitat. Conversely, if snow precipitation remains the same or decreases, as projected for the spring season by Hezel, Zhang, Bitz, Kelly, and Massonnet (2012), our findings suggest increased spatial coverage of suitable habitat. Regardless of the future snow situation, there will be one inevitable difference: the permanent and reliable ice-algal habitat found under springtime MYI will be replaced by a continuously varying habitat under springtime FYI.

The underestimation of the potential for MYI to host ice algae implies that the baseline for future predictions of ecosystem productivity and structure may be considerably higher than commonly assumed. Hence, relative increases in primary and secondary production due to a replacement of MYI by FYI may be lower than expected or even zero. Shifts in the timing of ice algae blooms caused by the different bloom dynamics in MYI vs. FYI, in addition to the presence of reliable ice-algal habitat in the form of MYI hummocks, however, may affect species which have adapted their life cycles to survival in hitherto MYI-dominated regions. Many key Arctic species (e.g., copepods, amphipods, polar cod and seals) have demonstrated a high dependency on ice algae derived carbon in almost all regions of the Arctic Ocean (e.g., Budge et al., 2008; Kohlbach et al., 2016, 2017; Sørdeide et al., 2013; Wang et al., 2015, 2016). Therefore, we suggest that the disappearance of MYI will have profound pan-Arctic ecological consequences yet to be fully understood and requires more extensive research efforts in the MYI-covered central Arctic Ocean.

ACKNOWLEDGEMENTS

We thank the logistical support from Jim Milne and Al Tremblay, Defense Research and Development-Atlantic. We thank G. Stewart and all of the personnel at Canadian Forces Station Alert for their hospitality and support. Invaluable logistical support, laboratory access and Helicopter and Twin Otter aircraft transportation were provided by the Polar Continental Shelf Program. Pilots from Universal Helicopters and Kenn Borek Air provided safe transportation throughout the project. We thank S. Duerksen, N. Fortin, K. Hille, G. Meisterhans, A. Niemi, M. Poulin, A. Tatare and J. Wiktor for their help in the field laboratory. This study was supported by the Alberta Ingenuity Scholarship Programme (RN:200700172) to CH, NSERC Discovery Grants to CH (356589-08) and CM, and the Canadian Federal Programme on Energy Research and Development to CM. BAL, JB, JAC and IH were supported by the Northern Scientific Training Program (NSTP) and Circumpolar-Boreal Arctic Research (C-BAR) Programme. This study is part of the Helmholtz Association Young Investigators Group *Iceflux*: ice-ecosystem carbon flux in polar oceans (VH-NG-800). We also acknowledge Fisheries and Oceans Canada and the Alfred-Wegener-Institut, Helmholtz-Zentrum für Polar- und Meeresforschung for additional financial support. Processing of the CryoSat-2 (ice thickness data) is funded by the German Ministry of Economics Affairs and Energy (grant: 50EE1008). Data from April 2013 was obtained from

<http://www.meereisportal.de> (grant: REKLIM-2013-04). We acknowledge M. Nicolaus and C. Katlein for helpful discussions in regard to the calculation of transmittance.

REFERENCES

- Barlow, R. G., Gosselin, M., Legendre, L., Therriault, J. C., Demers, S., Mantoura, R. F. C., & Llewellyn, C. A. (1988). Photoadaptive strategies in sea-ice microalgae. *Marine Ecology Progress Series*, *45*, 145–152.
- Budge, S. M., Wooller, M. J., Springer, A. M., Iverson, S. J., Mcroy, C. P., & Divoky, G. J. (2008). Tracing carbon flow in an arctic marine food web using fatty acid-stable isotope analysis. *Oecologia*, *157*, 117–129.
- Dunne, J. P., John, J. G., Adcroft, A. J., Griffies, S. M., Hallberg, R. W., Shevliakova, E., ... Zadeh, N. (2012). GFDL's ESM2 global coupled climate-carbon earth system models. Part I: Physical formulation and baseline simulation characteristics. *Journal of Climate*, *25*, 6646–6665.
- Dupont, F. (2012). Impact of sea-ice biology on overall primary production in a biophysical model of the pan-Arctic Ocean. *Journal of Geophysical Research*, *117*, C00D17. <https://doi.org/10.1029/2011jc006983>
- Eastwood, S. (2012). *OSI SAF sea ice product manual*, v3.8 edn. Oslo, Norway: Norwegian Meteorological Institute. Available at: <http://osisaf.met.no>
- Fernández-Méndez, M., Katlein, C., Rabe, B., Nicolaus, M., Peeken, I., Bakker, K., ... Boetius, A. (2015). Photosynthetic production in the Central Arctic during the record sea-ice minimum in 2012. *Biogeosciences*, *12*, 2897–2945.
- Gosselin, M., Legendre, L., Demers, S., & Ingram, R. G. (1985). Responses of sea-ice microalgae to climatic and fortnightly tidal energy inputs (Manitounuk Sound, Hudson Bay). *Canadian Journal of Fisheries and Aquatic Sciences*, *42*, 999–1006.
- Gosselin, M., Legendre, L., Therriault, J. C., Demers, S., & Rochet, M. (1986). Physical control of the horizontal patchiness of sea-ice microalgae. *Marine Ecology Progress Series*, *29*, 289–298.
- Gosselin, M., Levasseur, M., Wheeler, P. A., Horner, R. A., & Booth, B. C. (1997). New measurements of phytoplankton and ice algal production in the Arctic Ocean. *Deep Sea Research Part II: Topical Studies in Oceanography*, *44*, 1623–1644.
- Granskog, M. A., Kaartokallio, H., Kuosa, H., Thomas, D. N., Ehn, J., & Sonninen, E. (2005). Scales of horizontal patchiness in chlorophyll a, chemical and physical properties of landfast sea ice in the Gulf of Finland (Baltic Sea). *Polar Biology*, *28*, 276–283.
- Grenfell, T. C., & Maykut, G. A. (1977). The optical properties of ice and snow in the Arctic Basin. *Journal of Glaciology*, *18*, 445–463.
- Haas, C., & Druckenmiller, M. (2009). Ice thickness and roughness measurements. In H. Eicken (Ed.), *Field techniques for sea ice research* (pp. 565). Fairbanks: University of Alaska Press.
- Haas, C., & Eicken, H. (2001). Interannual variability of summer sea ice thickness in the Siberian and central Arctic under different atmospheric circulation regimes. *Journal of Geophysical Research*, *106*, 4449–4462.
- Haas, C., Hendricks, S., & Doble, M. (2006). Comparison of the sea-ice thickness distribution in the Lincoln Sea and adjacent Arctic Ocean in 2004 and 2005. *Annals of Glaciology*, *44*, 247–252.
- Haas, C., Hendricks, S., Eicken, H., & Herber, A. (2010). Synoptic airborne thickness surveys reveal state of Arctic sea ice cover. *Geophysical Research Letters*, *37*, L09501. <https://doi.org/10.1029/2010GL042652>
- Hatam, I., Lange, B., Beckers, J., Haas, C., & Lanoil, B. (2016). Bacterial communities from Arctic seasonal sea ice are more compositionally variable than those from multi-year sea ice. *ISME Journal*, *10*, 2543–2552. <https://doi.org/10.1038/ismej.2016.4>
- Hezel, P. J., Zhang, X., Bitz, C. M., Kelly, B. P., & Massonnet, F. (2012). Projected decline in spring snow depth on Arctic sea ice caused by progressively later autumn open ocean freeze-up this century. *Geophysical Research Letters*, *39*, L17505. <https://doi.org/10.1029/2012gl052794>
- Iacozza, J., & Barber, D. G. (1999). An examination of the distribution of snow on sea-ice. *Atmosphere-Ocean*, *37*, 21–51.
- IPCC (2013). *Climate Change 2013: The Physical Science Basis. Contribution of Working Group I to the Fifth Assessment Report of the Intergovernmental Panel on Climate Change*. In T. F. Stocker, D. Qin, G.-K. Plattner, M. Tignor, S. K. Allen, J. Boschung, A. Nauels, Y. Xia, V. Bex & P. M. Midgley (Eds.), *Climate change 2013: The physical basis*. (pp. 1535). Cambridge, UK and New York, NY, USA: Cambridge University Press.
- Juhl, A. R., & Krembs, C. (2010). Effects of snow removal and algal photoacclimation on growth and export of ice algae. *Polar Biology*, *33*, 1057–1065.
- Katlein, C., Arndt, S., Nicolaus, M., Perovich, D. K., Jakuba, M. V., Suman, S., ... German, C. R. (2015). Influence of ice thickness and surface properties on light transmission through Arctic sea ice. *Journal of Geophysical Research: Oceans*, *120*, 5932–5944.
- Katlein, C., Fernández-Méndez, M., Wenzhöfer, F., & Nicolaus, M. (2014). Distribution of algal aggregates under summer sea ice in the Central Arctic. *Polar Biology*, *38*, 719–731. <https://doi.org/10.1007/s00300-014-1634-3>
- Katlein, C., Perovich, D. K., & Nicolaus, M. (2016). Geometric effects of an inhomogeneous sea ice cover on the under ice light field. *Frontiers in Earth Science*, *4*, 1–10.
- Kohlbach, D., Graeve, M., Lange, B. A., David, C., Peeken, I., & Flores, H. (2016). The importance of ice algae-produced carbon in the central Arctic Ocean ecosystem: Food web relationships revealed by lipid and stable isotope analyses. *Limnology and Oceanography*, *61*, 2027–2044. <https://doi.org/10.1002/lno.10351>
- Kohlbach, D., Schaafsma, F. L., Graeve, M., Lebreton, B., Lange, B. A., David, C., ... Flores, H. (2017). Strong linkage of polar cod (*Boreogadus saida*) to sea ice algae-produced carbon: Evidence from stomach content, fatty acid and stable isotope analyses. *Progress in Oceanography*, *152*, 62–74. <https://doi.org/10.1016/j.pocean.2017.02.003>
- Kurtz, N. T., & Farrell, S. L. (2011). Large-scale surveys of snow depth on Arctic sea ice from Operation IceBridge. *Geophysical Research Letters*, *38*, L20505. <https://doi.org/10.1029/2011gl049216>
- Kwok, R., & Haas, C. (2015). Effects of radar side-lobes on snow depth retrievals from Operation IceBridge. *Journal of Glaciology*, *61*, 576–584.
- Kwok, R., & Rothrock, D. A. (2009). Decline in Arctic sea ice thickness from submarine and ICESat records: 1958–2008. *Geophysical Research Letters*, *36*, L15501. <https://doi.org/10.1029/2009GL039035>
- Lange, B. A., Katlein, C., Nicolaus, M., Peeken, I., & Flores, H. (2016). Sea ice algae chlorophyll a concentrations derived from under-ice spectral radiation profiling platforms. *Journal of Geophysical Research: Oceans*, *121*, 8511–8534. <https://doi.org/10.1002/2016JC011991>
- Lange, B. A., Michel, C., Beckers, J. F., Casey, J. A., Flores, H., Hatam, I., ... Haas, C. (2015). Comparing springtime ice-algal chlorophyll a and physical properties of multi-year and first-year sea ice from the Lincoln Sea. *PLoS ONE*, *10*, e0122418. <https://doi.org/10.1371/journal.pone.0122418>
- Laxon, S. W., Giles, K. A., Ridout, A. L., Wingham, D. J., Willatt, R., Cullen, R., ... Davidson, M. (2013). CryoSat-2 estimates of Arctic sea ice thickness and volume. *Geophysical Research Letters*, *40*, 732–737. <https://doi.org/10.1002/grl.50193>
- Legendre, L., Aota, M., Shirasawa, K., Martineau, M. J., & Ishikawa, M. (1991). Crystallographic structure of sea ice along a salinity gradient and environmental control of microalgae in the brine cells. *Journal of Marine Systems*, *2*, 347–357.
- Legendre, P., & Fortin, M.-J. (1989). Spatial Pattern and ecological analysis. *Vegetation*, *80*, 107–138.

- Maslanik, J. A., Stroeve, J. C., Fowler, C., & Emery, W. (2011). Distribution and trends in Arctic sea ice age through spring 2011. *Geophysical Research Letters*, 38, L13502. <https://doi.org/10.1029/2011GL047735>
- Maykut, G. A., & Grenfell, T. C. (1975). Spectral distribution of light beneath 1st-year sea ice in Arctic Ocean. *Limnology and Oceanography*, 20, 554–563.
- Melnikov, I. A., Kolosova, E. G., Welch, H. E., & Zhitina, L. S. (2002). Sea ice biological communities and nutrient dynamics in the Canada Basin of the Arctic Ocean. *Deep Sea Research Part I: Oceanographic Research Papers*, 49, 1623–1649.
- Michel, C., Legendre, L., Demers, S., & Therriault, J. (1988). Photoadaptation of sea-ice microalgae in springtime: Photosynthesis and carboxylating enzymes. *Marine Ecology Progress Series*, 50, 177–185.
- Moran, P. A. (1950). Notes on continuous stochastic phenomena. *Biometrika*, 37, 17–23.
- Mundy, C., Barber, D., & Michel, C. (2005). Variability of snow and ice thermal, physical and optical properties pertinent to sea ice algae biomass during spring. *Journal of Marine Systems*, 58, 107–120. <https://doi.org/10.1016/j.jmarsys.2005.07.003>
- Newman, T., Farrell, S. L., Richter-Menge, J., Connor, L. N., Kurtz, N. T., Elder, B. C., & Mcadoo, D. (2014). Assessment of radar-derived snow depth over Arctic sea ice. *Journal of Geophysical Research: Oceans*, 119, 8578–8602. <https://doi.org/10.1002/2014jc010284>
- Nicolaus, M., Hudson, S. R., Gerland, S., & Munderloh, K. (2010). A modern concept for autonomous and continuous measurements of spectral albedo and transmittance of sea ice. *Cold Regions Science and Technology*, 62, 14–28.
- Parkinson, C. L., & Comiso, J. C. (2013). On the 2012 record low Arctic sea ice cover: Combined impact of preconditioning and an August storm. *Geophysical Research Letters*, 40, 1356–1361. <https://doi.org/10.1002/grl.50349>
- Parsons, T. R., Maita, Y., & Lalli, C. M. (1989). *A manual of chemical and biological methods for seawater analysis*. Toronto: Pergamon Press.
- Perovich, D. K. (1996). The optical properties of sea ice, Rep. 96-1., Cold Regions Research and Engineering Laboratory.
- Perovich, D. K., Grenfell, T. C., Richter-Menge, J. A., Light, B., Tucker Iii, W. B., & Eicken, H. (2003). Thin and thinner: Sea ice mass balance measurements during SHEBA. *Journal of Geophysical Research*, 108, <https://doi.org/10.1029/2001JC001079>
- R-Development-Core-Team (2012). *R: A language and environment for statistical computing*. Vienna, Austria: R Foundation for Statistical Computing.
- Ricker, R., Hendricks, S., Helm, V., Skourup, H., & Davidson, M. (2014). Sensitivity of CryoSat-2 Arctic sea-ice freeboard and thickness on radar-waveform interpretation. *The Cryosphere*, 8, 1607–1622.
- Rysgaard, S., Kühl, M., Glud, R. N., & Hansen, J. W. (2001). Biomass, production and horizontal patchiness of sea ice algae in a high-Arctic fjord (Young Sound, NE Greenland). *Marine Ecology Progress Series*, 223, 15–26.
- Schünemann, H., & Werner, I. (2005). Seasonal variations in distribution patterns of sympagic meiofauna in Arctic pack ice. *Marine Biology*, 146, 1091–1102.
- Schweiger, A., Lindsay, R., Zhang, J., Steele, M., Stern, H., & Kwok, R. (2011). Uncertainty in modeled Arctic sea ice volume. *Journal of Geophysical Research*, 116, C00D06. <https://doi.org/10.1029/2011jc007084>
- Søgaard, D. H., Kristensen, M., Rysgaard, S., Glud, R. N., Hansen, P. J., & Hilligsøe, K. M. (2010). Autotrophic and heterotrophic activity in Arctic first-year sea ice: Seasonal study from Malene Bight, SW Greenland. *Marine Ecology Progress Series*, 419, 31–45.
- Sørdeide, J. E., Carroll, M. L., Hop, H., Ambrose, W. G., Hegseth, E. N., & Falk-Petersen, S. (2013). Sympagic-pelagic-benthic coupling in Arctic and Atlantic waters around Svalbard revealed by stable isotopic and fatty acid tracers. *Marine Biology Research*, 9, 831–850.
- Stroeve, J. C., Kattsov, V., Barrett, A., Serreze, M., Pavlova, T., Holland, M., & Meier, W. N. (2012). Trends in Arctic sea ice extent from CMIP5, CMIP3 and observations. *Geophysical Research Letters*, 39, L16502. <https://doi.org/10.1029/2012GL052676>
- Stroeve, J. C., Serreze, M. C., Holland, M. M., Kay, J. E., Malanik, J., & Barrett, A. P. (2011). The Arctic's rapidly shrinking sea ice cover: A research synthesis. *Climatic Change*, 110, 1005–1027. <https://doi.org/10.1007/s10584-011-0101-1>
- Sturm, M., Holmgren, J., & Perovich, D. K. (2002). Winter snow cover on the sea ice of the Arctic Ocean at the Surface Heat Budget of the Arctic Ocean (SHEBA): Temporal evolution and spatial variability. *Journal of Geophysical Research*, 107, C108047. <https://doi.org/10.1029/2000JC000400>
- Thomas, C. W. (1963). On the transfer of visible radiation through sea ice and snow. *Journal of Glaciology*, 4, 481–484.
- Toms, J. D., & Lesperance, M. L. (2003). Piecewise regression: A tool for identifying ecological thresholds. *Ecology*, 84, 2034–2041.
- Toms, J. D., & Villard, M.-A. (2015). Threshold detection: Matching statistical methodology to ecological questions and conservation planning objectives. *Avian Conservation and Ecology*, 10, 1–8.
- Vancoppenolle, M., Bopp, L., Madec, G., Dunne, J., Ilyina, T., Halloran, P. R., & Steiner, N. (2013). Future Arctic Ocean primary productivity from CMIP5 simulations: Uncertain outcome, but consistent mechanisms. *Global Biogeochemical Cycles*, 27, 605–619.
- Vancoppenolle, M., Meiners, K. M., Michel, C., Bopp, L., Brabant, F., Carnat, G., . . . Moreau, S. (2013). Role of sea ice in global biogeochemical cycles: Emerging views and challenges. *Quaternary Science Reviews*, 79, 207–230. <https://doi.org/10.1016/j.quascirev.2013.04.011>
- Wang, S. W., Budge, S. M., Iken, K., Gradinger, R. R., Springer, A. M., & Wooller, M. J. (2015). Importance of sympagic production to Bering Sea zooplankton as revealed from fatty acid-carbon stable isotope analyses. *Marine Ecology Progress Series*, 518, 31–50.
- Wang, S. W., Springer, A. M., Budge, S. M., Horstmann, L., Quakenbush, L. T., & Wooller, M. J. (2016). Carbon sources and trophic relationships of ice seals during recent environmental shifts in the Bering Sea. *Ecological Applications*, 26, 830–845.
- Warren, S. G., Rigor, I. G., Untersteiner, N., Radionov, V. F., Bryazgin, N. N., Aleksandrov, Y. I., & Colony, R. (1999). Snow depth on arctic sea ice. *Journal of Climate*, 12, 1814–1829.
- Wassmann, P. (2011). Arctic marine ecosystems in an era of rapid climate change. *Progress in Oceanography*, 90, 1–17. <https://doi.org/10.1016/j.pocean.2011.02.002>
- Wassmann, P., Duarte, C. M., Agusti, S., & Sejr, M. K. (2011). Footprints of climate change in the Arctic marine ecosystem. *Global Change Biology*, 17, 1235–1249. <https://doi.org/10.1111/j.1365-2486.2010.02311.x>
- Weissling, B. P., Lewis, M. J., & Ackley, S. F. (2011). Sea-ice thickness and mass at Ice Station Belgica, Bellingshausen Sea, Antarctica. *Deep Sea Research Part II: Topical Studies in Oceanography*, 58, 1112–1124.

SUPPORTING INFORMATION

Additional Supporting Information may be found online in the supporting information tab for this article.

How to cite this article: Lange BA, Flores H, Michel C, et al. Pan-Arctic sea ice-algal chl *a* biomass and suitable habitat are largely underestimated for multiyear ice. *Glob Change Biol*. 2017;00:1–17. <https://doi.org/10.1111/gcb.13742>